

NGU Report 2014.052

Helicopter-borne magnetic, electromagnetic and radiometric geophysical survey in the Hjarthdal-Rjukan-Flesberg area, Telemark and Buskerud.

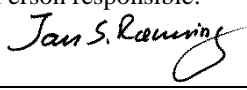
Report no.: 2014.052		ISSN 0800-3416	Grading: Open
Title: Helicopter-borne magnetic, electromagnetic and radiometric geophysical survey in the Hjartdal-Rjukan-Flesberg area, Telemark and Buskerud.			
Authors: Alexei Rodionov, Frode Ofstad, Alexandros Stampolidis & Georgios Tassis.		Client: NGU	
County: Telemark and Buskerud		Municipalities: Hjartdal, Tinn, Notodden, Rollag og Flesberg	
Map-sheet name (M=1:250.000) SKIEN		Map-sheet no. and -name (M=1:50.000) 1614 I Tinnsjø, 1614 II Gransherad, 1614 III Flatdal. 1614 IV Rjukan, 1714 III Notodden, 1714 IV Flesberg	
Deposit name and grid-reference: Tinnoset UTM 32 W 501800 – 6620800		Number of pages: 29 Price (NOK): 120,- Map enclosures:	
Fieldwork carried out: October-November 2013 October-November 2014	Date of report: December 2014	Project no.: 342900	Person responsible: 
Summary: <p>NGU conducted an airborne geophysical survey in the Hjartdal-Rjukan-Flesberg area area in October-November 2013, October-November 2014 as a part of the MINS project. This report describes and documents the acquisition, processing and visualization of recorded datasets. The geophysical survey results reported herein are 9700 line km, covering an area of 1940 km².</p> <p>The NGU modified Geotech Ltd. Hummingbird frequency domain system supplemented by optically pumped Cesium magnetometer and a 1024 channels RSX-5 spectrometer was used for data acquisition.</p> <p>The survey was flown with 200 m line spacing, line direction 320° (Northeast to Southwest), 140° (Northwest to Southeast) and average speed 74 km/h. The average terrain clearance of the bird was 57 m.</p> <p>Collected data were processed by AR Geoconsulting using Geosoft Oasis Montaj software. Raw total magnetic field data were corrected for diurnal variation and levelled using standard micro levelling algorithm. Final grid was filtered using Butterworth filter.</p> <p>EM data were filtered and levelled using both automated and manual levelling procedure. Apparent resistivity was calculated from in-phase and quadrature data for two high frequencies (6606 and 7001 Hz), separately using homogeneous half space model. Apparent resistivity grids were filtered using 3x3 convolution filter. Resistivity was not calculated for low frequencies (880 and 980 Hz) due to low signal/noise ratio and survey results presented as profile plots of in-phase and quadrature responses.</p> <p>Radiometric data were processed using standard procedures recommended by International Atomic Energy Association.</p> <p>Data were gridded with the cell size of 50 x 50 m and presented as a shaded relief maps at the scale of 1:50000.</p>			
Keywords: Geophysics		Airborne	Magnetic
Electromagnetic		Gamma spectrometry	Radiometric
			Technical report

Table of Contents

1. INTRODUCTION	4
2. SURVEY SPECIFICATIONS	5
2.1 Airborne Survey Parameters.....	5
2.2 Airborne Survey Instrumentation	6
2.3 Airborne Survey Logistics Summary	6
3. DATA PROCESSING AND PRESENTATION	7
3.1 Total Field Magnetic Data	7
3.2 Electromagnetic Data	9
3.3 Radiometric data	10
4. PRODUCTS.....	14
5. REFERENCES	15
Appendix A1: Flow chart of magnetic processing.....	16
Appendix A2: Flow chart of EM processing.....	16
Appendix A3: Flow chart of radiometry processing.....	16

FIGURES

Figure 1: Hjarthdal-Rjukan-Flesberg area survey area.....	4
Figure 2: Hummingbird system in air	7
Figure 3: Gamma-ray spectrum with the K, Th, U and Total count windows.....	10
Figure 4: Notodden survey area with flight path	19
Figure 5: Total Magnetic Field	20
Figure 6: Magnetic Vertical Derivative.....	21
Figure 7: Magnetic Tilt Derivative	22
Figure 8: Apparent resistivity. Frequency 6600 Hz, Coplanar coils	23
Figure 9: In-phase and quadrature response. Frequency 880 Hz, coplanar coils.....	24
Figure 10: Apparent resistivity. Frequency 7000 Hz, Coaxial coils	25
Figure 11: In-phase and quadrature response. Frequency 980 Hz, Coaxial coils.....	26
Figure 12: Uranium ground concentration.....	27
Figure 13: Thorium ground concentration	28
Figure 14: Potassium ground concentration.....	29
Figure 15: Radiometric Ternary map	30

TABLES

Table 1. Instrument Specifications	6
Table 2. Hummingbird electromagnetic system, frequency and coil configurations.....	6
Table 3: Specified channel windows and energy spectrum for the RSX-5 systems used in this survey	11
Table 4. Maps in scale 1:50000 available from NGU on request.	14

1. INTRODUCTION

In 2013 the Norwegian government initiated a new program for mapping of mineral resources in Southern Norway (MINS). The goal of this program is to enhance the geological information that is relevant to an assessment of the mineral potential of the southernmost mainland Norway. The airborne geophysical surveys - helicopter borne and fixed wing- are important integral part of MINS program. The airborne survey results reported herein amount to 9700 line km (1940 km²) over the Hjartdal-Rjukan-Flesberg area, as shown in **Figure 1**.

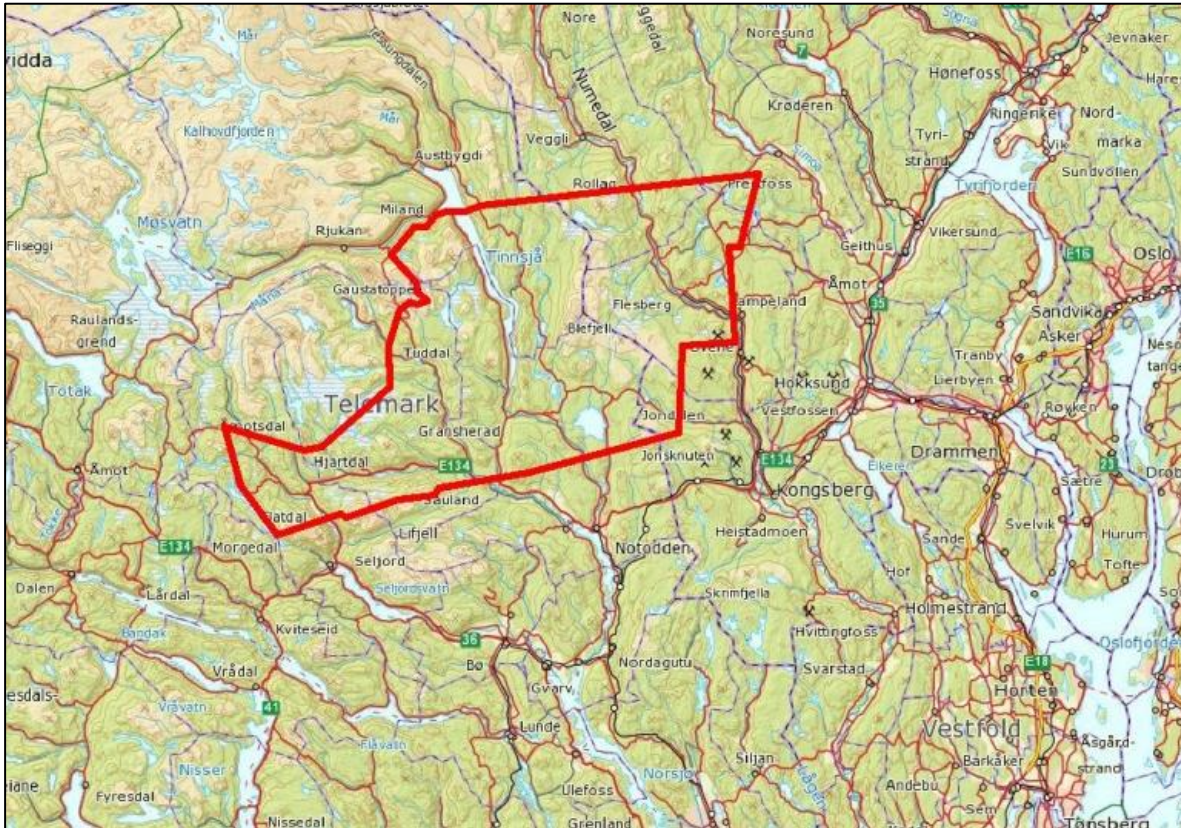


Figure 1: Hjartdal-Rjukan-Flesberg area survey area

The objective of the airborne geophysical survey was to obtain a dense high-resolution aeromagnetic, electromagnetic and radiometric data over the survey area. This data is required for the enhancement of a general understanding of the regional geology of the area. In this regard, the data can also be used to map contacts and structural features within the property. It also improves defining the potential of known zones of mineralization, their geological settings, and identifying new areas of interest.

The survey incorporated the use of a Hummingbird™ five-frequency electromagnetic system supplemented by a high-sensitivity caesium magnetometer, gamma-ray spectrometer and radar altimeter. A GPS navigation computer system with flight path indicators ensured accurate positioning of the geophysical data with respect to the World Geodetic System 1984 geodetic datum (WGS-84).

2. SURVEY SPECIFICATIONS

2.1 Airborne Survey Parameters

NGU used a modified Hummingbird™ electromagnetic and magnetic helicopter survey system designed to obtain low level, slow speed, detailed airborne magnetic and electromagnetic data (Geotech 1997). The system was supplemented by 1024 channel gamma-ray spectrometer which was used to map ground concentrations of U, Th and K.

The airborne survey began on October 16th 2013 and was cancelled on November 11th due to bad weather. It was continued on October 12th 2014 and completed on November 5th 2014. A Eurocopter AS350-B3 helicopter from helicopter company HeliScan AS was used to tow the bird. The survey lines were spaced 200 m apart. Lines were oriented at a 140° azimuth (UTM zone 32W coordinates).

The magnetic and electromagnetic sensors are housed in a single 7.5 m long bird, which was maintained at an average of 57 m above the topographic surface. A gamma-ray spectrometer, installed under the belly of the helicopter, registered natural gamma ray radiation simultaneously with the acquisition of magnetic/EM data.

Just before the start of the first survey of 2014 field season, instrumental problems were discovered. The highest frequency (34 kHz) was not stable, and this instability influenced on the quality of the other frequencies. To be able to collect data for the four lowest frequencies, it was decided not to transmit on 33.4 kHz.

Rugged terrain and abrupt changes in topography affected the aircraft pilot's ability to 'drape' the terrain; therefore the average instrumental height was higher than the standard survey instrumental height, which is defined as 30 m plus a height of obstacles (trees, power lines etc.) for EM and magnetic sensors.

The ground speed of the aircraft varied from 35 – 110 km/h depending on topography, wind direction and its magnitude. On average, the ground speed during measurements is calculated to 74 km/h. Magnetic data were recorded at 0.2 second intervals resulting in approximately 4 m point spacing. EM data were recorded at 0.1 second intervals resulting in data with a sample increment of 2 m along the ground in average. Spectrometry data were recorded every 1 second giving a point spacing of approximately 20 meters. The above parameters allow recognizing sufficient detail in the data to detect subtle anomalies that may represent mineralization and/or rocks of different lithological and petrophysical composition.

A base magnetometer to monitor diurnal variations in the magnetic field was located at Notodden (UTM 510500 – 6602800) in 2013 and at Jondalen (UTM 531200 – 6619200) in 2014. GEM GSM-19 station magnetometer data were recorded once every 3 seconds. The CPU clock of the base magnetometer and the helicopter magnetometer were both synchronized to UTC (Universal Time Coordinates) through the built-in GPS receiver to allow correction of diurnals.

Navigation system uses GPS/GLONASS satellite tracking systems to provide real-time WGS-84 coordinate locations for every second. The accuracy achieved with no differential corrections is reported to be less than ± 5 m in the horizontal directions. The GPS receiver antenna was mounted externally to the tail tip of the helicopter.

For quality control, the electromagnetic, magnetic and radiometric, altitude and navigation data were monitored on four separate windows in the operator's display during flight while they were recorded in three data ASCII streams to the PC hard disk drive. Spectrometry data were also recorded to an internal hard drive of the spectrometer. The data files were transferred to the field workstation via USB flash drive. The raw data files were backed up onto USB flash drive in the field.

2.2 Airborne Survey Instrumentation

Instrument specification is given in table 1. Frequencies and coil configuration for the Hummingbird EM system is given in table 2.

Table 1. Instrument Specifications

Instrument	Producer/Model	Accuracy	Sampling frequency/interval
Magnetometer	Scintrex Cs-2	0,002 nT	5 Hz
Base magnetometer	GEM GSM-19	0.1 nT	3 sec
Electromagnetic	Geotech Hummingbird	1 – 2 ppm	10 Hz
Gamma spectrometer	Radiation Solutions RSX-5	1024 channels, 16 liters down, 4 liters up	1 Hz
Radar altimeter	Bendix/King KRA 405B	± 3 % 0 – 500 feet ± 5 % 500 – 2500 feet	1 Hz
Pressure/temperature	Honeywell PPT	± 0,03 % FS	1 Hz
Navigation	Topcon GPS-receiver	± 5 meter	1 Hz
Acquisition system	PC based in house software		

Table 2. Hummingbird electromagnetic system, frequency and coil configurations

Coils:	Frequency	Orientation	Separation
A	7700 Hz	Coaxial	6.20 m
B	6600 Hz	Coplanar	6.20 m
C	980 Hz	Coaxial	6.025 m
D	880 Hz	Coplanar	6.025 m

2.3 Airborne Survey Logistics Summary

Traverse (survey) line spacing:	200 metres
Traverse line direction:	140° NE-SW
Nominal aircraft ground speed:	30 - 110 km/h
Average sensor terrain clearance EM+Mag:	57 metres
Average sensor terrain clearance Rad:	87 metres
Sampling rates:	0.2 seconds - magnetometer 0.1 seconds - electromagnetics 1.0 second - spectrometer, GPS, altimeter



Figure 2: Hummingbird system in air

3. DATA PROCESSING AND PRESENTATION

All data were processed by Alexei Rodionov (AR Geoconsulting Ltd., Canada) in Calgary. The ASCII data files were loaded into three separate Oasis Montaj databases. All three datasets were processed consequently according to processing flow charts shown in Appendix A1, A2 and A3.

3.1 Total Field Magnetic Data

At the first stage the raw magnetic data were visually inspected and spikes were removed manually. Non-linear filter was also applied to airborne raw data to eliminate short-period spikes.

Typically, several corrections have to be applied to magnetic data before gridding - heading correction, lag correction and diurnal correction.

Diurnal Corrections

The temporal fluctuations in the magnetic field of the earth affect the total magnetic field readings recorded during the airborne survey. This is commonly referred to as the magnetic diurnal variation. These fluctuations can be effectively removed from the airborne magnetic dataset by using a stationary reference magnetometer that records the magnetic field of the earth simultaneously with the airborne sensor at given short time interval in the neighbourhood of the survey area. The data from base station were imported in database using the standard Oasis magbase.gx module. Diurnal variation channel was inspected for spikes

and spikes were removed manually if necessary. Magnetic diurnals data were within the standard NGU specifications during the entire survey (Rønning 2013).

Diurnal variations were measured with GEM GSM-19 magnetometer. The recorded data are merged with the airborne data and the diurnal correction is applied according to equation (1).

$$\mathbf{B}_{Tc} = \mathbf{B}_T + (\bar{\mathbf{B}}_B - \mathbf{B}_B), \quad (1)$$

where:

\mathbf{B}_{Tc} = Corrected airborne total field readings

\mathbf{B}_T = Airborne total field readings

$\bar{\mathbf{B}}_B$ = Average datum base level

\mathbf{B}_B = Base station readings

Corrections for Lag and heading

Neither a lag nor cloverleaf tests were performed before the survey. According to previous reports the lag between logged magnetic data and the corresponding navigational data was 1-2 fids. Translated to a distance it would be no more than 10 m - the value comparable with the precision of GPS. A heading error for a towed system is usually either very small or non-existent. So no lag and heading corrections were applied.

Magnetic data processing, gridding and presentation

The total field magnetic anomaly data (\mathbf{B}_{TA}) were calculated from the diurnal corrected data (\mathbf{B}_{Tc}) after subtracting the IGRF for the surveyed area calculated for the data period (eq.2)

$$\mathbf{B}_{TA} = \mathbf{B}_{Tc} - IGRF \quad (2)$$

The total field anomaly data were gridded using a minimum curvature method with a grid cell size of 50 meters. This cell size is equal to one quarter of the 200 m average line spacing. In order to remove small line-to-line levelling errors that were detected on the gridded magnetic anomaly data, the Geosoft Micro-levelling technique was applied on the flight line based magnetic database. Then, the micro-levelled channel was gridded using again a minimum curvature method with 50 m grid cell size. Finally, Butterworth filter was applied to reduce “ringing” effect of gridding and smooth the grid.

The processing steps of magnetic data presented so far, were performed on point basis. The following steps are performed on grid basis. Vertical Gradient along with the Tilt Derivative of the total magnetic anomaly was calculated from the micro-levelled total magnetic anomaly grid. The Tilt derivative (TD) was calculated according to the equation (3)

$$TD = \tan^{-1} \left(\frac{VG}{HG} \right) \quad (3)$$

The results are presented in coloured shaded relief maps:

- A. Total field magnetic anomaly
- B. Vertical gradient of total magnetic anomaly
- C. Tilt angle (or Tilt Derivative) of the total magnetic anomaly

These maps are representative of the distribution of magnetization over the surveyed areas. The list of the produced maps is shown in **Table 4**.

3.2 Electromagnetic Data

The DAS computer records both an in-phase and a quadrature value for each of the four coil sets of the electromagnetic system. Instrumental noise and drift should be removed before computation of an apparent resistivity.

Instrumental noise

Noise level on all frequencies was above the survey specification during the whole survey. Partially it was the result of swaying of the bird. The pendulum effect of a swaying was clear visible on records especially on 880 Hz data. Presence of numerous habitations and power lines introduced so called “cultural noise” which especially affected high frequencies. Lastly, electronics malfunction also contributed to elevation of noise level. Traditionally used combination of short non-linear filter and low pass filter could not suppress the noise. The period of bird swaying – 3-8 sec. made application of low pass filter not effective. Low pass filter, eliminating noise, also distorted a shape and amplitude of anomalies. To achieve satisfactory results, spline approximation (B-spline filter) was applied to all data. Parameters of filter were individually chosen for each flight and sometimes for separate lines.

Shifts of 7000 Ip and Q records, with amplitude of 15-20 ppm, was observed almost in all flights, especially, in mountainous areas. Shifts were edited manually where it was possible.

Instrument Drift

In order to remove the effects of instrument drift caused by gradual temperature variations in the transmitting and receiving circuits, background responses are recorded during each flight. To obtain a background level the bird is raised to an altitude of at least 1000 ft above the topographic surface so that no electromagnetic responses from the ground are present in the recorded traces. The EM traces observed at this altitude correspond to a background (zero) level of the system. If these background levels are recorded at 20-30 minute intervals, then the drift of the system (assumed to be linear) can be removed from the data by resetting these points to the initial zero level of the system. The drift must be removed on a flight-by-flight basis, before any further processing is carried out. Geosoft HEM module was used for applying drift correction. Residual instrumental drift, usually small, but non-linear, was manually removed on line-to-line basis.

Instrumental drift during this survey was non-linear even in short time (3-5 min) intervals and not within specifications (Rønning 2013) due to malfunction of Hummingbird electronics.

Apparent resistivity calculation and presentation

When levelling of the EM data was complete, apparent resistivity was calculated from in-phase and quadrature EM components using a homogeneous half space model of the Earth (Geosoft HEM module) for four frequencies 6600 and 7000 Hz. A threshold value of 1 ppm was set for inversion. Due to low signal to noise ratio, resistivity for 880 and 980 Hz was not calculated. The 880 and 980 Hz data are presented as profile plots of in-phase and quadrature responses. Note: Negative readings of in-phase component are controlled by high magnetic susceptibility of rocks. 34000 Hz data covers only part of the survey area (2013 year survey) and its results are not included in this report.

Secondary electromagnetic field decays rapidly with the distance (height of the sensors) – as $z^{-2} - z^{-5}$ depending on the shape of the conductors and, at certain height, signals from the ground sources become comparable with instrumental noise. Levelling errors or precision of levelling can lead sometimes to appearance of artificial resistivity anomalies when data were collected at high instrumental altitude. Application of threshold allows excluding such data from an apparent resistivity calculation, though not completely. It's particularly noticeable in low frequencies datasets. Resistivity data were visually inspected; artificial anomalies associated with high altitude measurements were manually removed.

Data, recorded at the height above 100 m were considered as non-reliable and removed from presentation. Remaining resistivity data were gridded with a cell size 50 m and 3x3 convolution filter was applied to smooth resistivity grids.

3.3 Radiometric data

Airborne gamma-ray spectrometry measures the abundance of Potassium (K), Thorium (eTh), and Uranium (eU) in rocks and weathered materials by detecting gamma-rays emitted due to the natural radioelement decay of these elements. The data analysis method is based on the IAEA recommended method for U, Th and K (International Atomic Energy Agency, 1991; 2003). A short description of the individual processing steps of that methodology as adopted by NGU is given below:

Energy windows

The Gamma-ray spectra were initially reduced into standard energy windows corresponding to the individual radio-nuclides K, U and Th. **Figure 3** shows an example of a Gamma-ray spectrum and the corresponding energy windows and radioisotopes (with peak energy in MeV) responsible for the radiation.

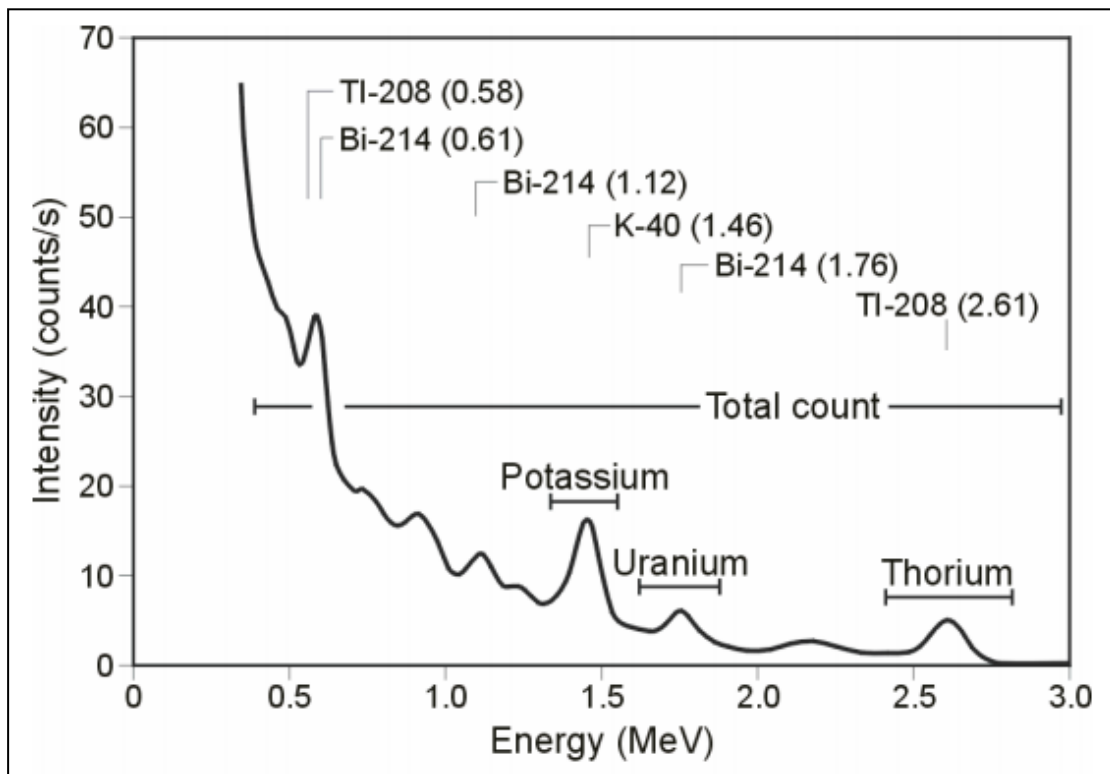


Figure 3: Gamma-ray spectrum with the K, Th, U and Total count windows.

The RSX-5 is a 1024 channel system with four downward and one upward looking detectors and the actual Gamma-ray spectrum is divided into 1024 channels. The first channel is reserved for the “Live Time” and the last for the Cosmic rays. **Table 3** shows the channels that were used for the reduction of the spectrum.

Table 3: Specified channel windows and energy spectrum for the RSX-5 systems used in this survey

Gamma-ray spectrum	Cosmic	Total count	K	U	Th
Down	1022	134-934	454-521	551-617	801-934
Up	1022			551-617	
Energy windows (MeV)	>3.07	0.41-2.81	1.37-1.57	1.66-1.86	2.41-2.81
Peak, keV			1460	1765	2614
Peak channel			486	586	872

Live Time correction

The data were corrected for live time. “Live time” is an expression of the relative period of time the instrument was able to register new pulses per sample interval. On the other hand “dead time” is an expression of the relative period of time the system was unable to register new pulses per sample interval. The relation between “dead” and “live time” is given by the equation (4)

$$\text{“Live time”} = \text{“Real time”} - \text{“Dead time”} \quad (4)$$

where the “real time” or “acquisition time” is the elapsed time over which the spectrum is accumulated (1 second).

The live time correction is applied to the total count, Potassium, Uranium, Thorium, upward Uranium and cosmic channels. The formula used to apply the correction is as follows:

$$C_{LT} = C_{RAW} \cdot \frac{1000000}{Live\ Time} \quad (5)$$

where C_{LT} is the live time corrected channel in counts per second, C_{RAW} is the raw channel data in counts per second and Live Time is in microseconds. To improve counting statistics, 5 fid low pass filter was applied to Uranium live time corrected data.

Cosmic and aircraft correction

Background radiation resulting from cosmic rays and aircraft contamination was removed from the total count, Potassium, Uranium, Thorium, upward Uranium channels using the following formula:

$$C_{CA} = C_{LT} - (a_c + b_c \cdot C_{Cos}) \quad (6)$$

where C_{CA} is the cosmic and aircraft corrected channel, C_{LT} is the live time corrected channel a_c is the aircraft background for this channel, b_c is the cosmic stripping coefficient for this channel and C_{Cos} is the low pass filtered cosmic channel.

Radon correction

The upward detector method, as discussed in IAEA (1991), was applied to remove the effects of the atmospheric radon in the air below and around the helicopter. Usages of over-water measurements where there is no contribution from the ground, enabled the calculation of the coefficients (a_c and b_c) of the linear equations that relate the cosmic corrected counts per

second of Uranium channel with total count, Potassium, Thorium and Uranium upward channels over water. Data over-land was used in conjunction with data over-water to calculate the a_1 and a_2 coefficients used in equation (7) for the determination of the Radon component in the downward uranium window:

$$Radon_U = \frac{U_{up_{CA}} - a_1 \cdot U_{CA} - a_2 \cdot Th_{CA} + a_2 \cdot b_{Th} - b_U}{a_U - a_1 - a_2 \cdot a_{Th}} \quad (7)$$

where $Radon_u$ is the radon component in the downward uranium window, $U_{up_{CA}}$ is the filtered upward uranium, U_{CA} is the filtered Uranium, Th_{CA} is the filtered Thorium, a_1 , a_2 , a_U and a_{Th} are proportional factors and b_U and b_{Th} are constants determined experimentally.

The effects of Radon in the downward Uranium are removed by simply subtracting $Radon_U$ from U_{CA} . The effects of radon in the other channels are removed using the following formula:

$$C_{RC} = C_{CA} - (a_C \cdot Radon_U + b_C) \quad (8)$$

where C_{RC} is the Radon corrected channel, C_{CA} is the cosmic and aircraft corrected channel, $Radon_U$ is the Radon component in the downward uranium window, a_C is the proportionality factor and b_C is the constant determined experimentally for this channel from over-water data.

Compton Stripping

Potassium, Uranium and Thorium Radon corrected channels, are subjected to spectral overlap correction. Compton scattered gamma rays in the radio-nuclides energy windows were corrected by window stripping using Compton stripping coefficients determined from measurements on calibrations pads at the Geological Survey of Norway in Trondheim (for values, see Appendix A3).

The stripping corrections are given by the following formulas:

$$A_1 = 1 - (g \cdot \gamma) - (a \cdot \alpha) + (a \cdot g \cdot \beta) - (b \cdot \beta) + (b \cdot \alpha \cdot \gamma) \quad (9)$$

$$U_{ST} = \frac{Th_{RC} \cdot ((g \cdot \beta) - \alpha) + U_{RC} \cdot (1 - b \cdot \beta) + K_{RC} \cdot ((b \cdot \alpha) - g)}{A_1} \quad (10)$$

$$Th_{ST} = \frac{Th_{RC} \cdot (1 - (g \cdot \gamma)) + U_{RC} \cdot (b \cdot \gamma - a) + K_{RC} \cdot ((a \cdot g) - b)}{A_1} \quad (11)$$

$$K_{ST} = \frac{Th_{RC} \cdot ((\alpha \cdot \gamma) - \beta) + U_{RC} \cdot ((a \cdot \beta) - \gamma) + K_{RC} \cdot (1 - (a \cdot \alpha))}{A_1} \quad (12)$$

where U_{RC} , Th_{RC} , K_{RC} are the radon corrected Uranium, Thorium and Potassium and a , b , g , α , β , γ are Compton stripping coefficients.

Reduction to Standard Temperature and Pressure

The radar altimeter data were converted to effective height (H_{STP}) using the acquired temperature and pressure data, according to the expression:

$$H_{STP} = H \cdot \frac{273.15}{T + 273.15} \cdot \frac{P}{1013.25} \quad (13)$$

where H is the smoothed observed radar altitude in meters, T is the measured air temperature in degrees Celsius and P is the measured barometric pressure in millibars.

Height correction

Variations caused by changes in the aircraft altitude relative to the ground was corrected to a nominal height of 60 m. Data recorded at the height above 150 m were considered as non-reliable and removed from processing. Total count, Uranium, Thorium and Potassium stripped channels were subjected to height correction according to the equation:

$$C_{60m} = C_{ST} \cdot e^{C_{ht}(60-H_{STP})} \quad (14)$$

where C_{ST} is the stripped corrected channel, C_{ht} is the height attenuation factor for that channel and H_{STP} is the effective height.

Conversion to ground concentrations

Finally, corrected count rates were converted to effective ground element concentrations using calibration values derived from calibration pads at the Geological Survey of Norway in Trondheim (for values, see Appendix A3). The corrected data provide an estimate of the apparent surface concentrations of Potassium, Uranium and Thorium (K, eU and eTh). Potassium concentration is expressed as a percentage, equivalent Uranium and Thorium as parts per million (ppm). Uranium and Thorium are described as “equivalent” since their presence is inferred from gamma-ray radiation from daughter elements (^{214}Bi for Uranium, ^{208}Tl for Thorium). The concentration of the elements is calculated according to the following expressions:

$$C_{CONC} = C_{60m} / C_{SENS_60m} \quad (15)$$

where C_{60m} is the height corrected channel, C_{SENS_60m} is experimentally determined sensitivity reduced to the nominal height (60m).

Spectrometry data gridding and presentation

Gamma-rays from Potassium, Thorium and Uranium emanate from the uppermost 30 to 40 centimetres of soil and rocks in the crust (Minty, 1997). Variations in the concentrations of these radioelements largely related to changes in the mineralogy and geochemistry of the Earth’s surface.

The spectrometry data were stored in a database and the ground concentrations were calculated following the processing steps. A list of the parameters used in these steps is given in Appendix A3.

Then the data were split in lines and ground concentrations of the three main natural radioelements Potassium, Thorium and Uranium and total gamma-ray flux (total count) were gridded using a minimum curvature method with a grid cell size of 50 meters. In order to remove small line-to-line levelling errors appeared on those grids, the data were micro-levelled as in the case of the magnetic data, and re-gridded with the same grid cell size. Finally, a 3x3 convolution filter was applied to Uranium grid to smooth the microlevelled concentration grids.

Quality of the radiometric data was within standard NGU specifications (Rønning 2013). For further reading regarding standard processing of airborne radiometric data, we recommend the publications from Minty et al. (1997).

4. PRODUCTS

Processed digital data from the survey are presented as:

1. Three Geosoft XYZ files:
Hjartdal-Rjukan-Flesberg-Mag.xyz, Hjartdal-Rjukan-Flesberg-EM.xyz,
Hjartdal-Rjukan-Flesberg-Rad.xyz
2. Georeferenced tiff files (Geo-tiff).
3. Maps in scale 1: 50.000 as jpg-files.

Table 4. Maps in scale 1:50000 available from NGU on request.

Map #	Name
2014.052-01	Total magnetic field
2014.052-02	Magnetic Vertical Derivative
2014.052-03	Magnetic Tilt Derivative
2014.052-04	Apparent resistivity, Frequency 6600 Hz, coplanar coils
2014.052-05	In-phase and quadrature response, Frequency 880 Hz, coplanar coils
2014.052-06	Apparent resistivity, Frequency 7000 Hz, coaxial coils
2014.052-07	In-phase and quadrature response, Frequency 980 Hz, coaxial coils
2014.052-08	Uranium ground concentration
2014.052-09	Thorium ground concentration
2014.052-10	Potassium ground concentration
2014.052-11	Radiometric Ternary Map

Downscaled images of the maps are shown on figures 4 to 15.

5. REFERENCES

- Geosoft 2010: Montaj MAGMAP Filtering, 2D-Frequency Domain Processing of Potential Field Data, Extension for Oasis Montaj v 7.1, Geosoft Corporation
- Grasty, R.L., Holman, P.B. & Blanchard 1991: Transportable Calibration pads for ground and airborne Gamma-ray Spectrometers. Geological Survey of Canada, Paper 90-23: 62 pp.
- IAEA 1991: Airborne Gamma-Ray Spectrometry Surveying, Technical Report No 323, Vienna, Austria, 97 pp.
- IAEA 2003: Guidelines for radioelement mapping using gamma ray spectrometry data. IAEA-TECDOC-1363, Vienna, Austria, 173 pp.
- Minty, B.R.S. 1997: The fundamentals of airborne gamma-ray spectrometry. AGSO Journal of Australian Geology and Geophysics, 17 (2): 39-50.
- Minty, B.R.S., Luyendyk, A.P.J. and Brodie, R.C. 1997: Calibration and data processing for gamma-ray spectrometry. AGSO Journal of Australian Geology and Geophysics, 17(2): 51-62.
- Naudy, H. and Dreyer, H. 1968: Non-linear filtering applied to aeromagnetic profiles. Geophysical Prospecting, 16(2): 171-178.
- Rønning, J.S. 2013: NGUs helikoptermålinger. Plan for sikring og kontroll av datakvalitet. NGU Intern rapport 2013.001, (38 sider).

Appendix A1: Flow chart of magnetic processing

Meaning of parameters is described in the referenced literature.

Processing flow:

- Quality control.
- Visual inspection of airborne data and manual spike removal
- Merge magbase data with EM database
- Import of diurnal data
- Correction of data for diurnal variation
- Splitting flight data by lines
- Gridding
- Microlevelling
- Butterworth filter

Appendix A2: Flow chart of EM processing

Meaning of parameters is described in the referenced literature.

Processing flow:

- Filtering of in-phase and quadrature channels with non-linear and low pass filters
- Selective application of B-spline filter to 880 Hz 7 kHz and 980 Hz data
- Automated leveling
- Quality control
- Visual inspection of data.
- Splitting flight data by lines
- Manual removal of remaining part of instrumental drift
- Calculation of an apparent resistivity using both - in-phase and quadrature channels
- Gridding
- 3x3 convolution filter

Appendix A3: Flow chart of radiometry processing

Underlined processing stages are not only applied to the K, U and Th window, but also to the total count.

Meaning of parameters is described in the referenced literature.

Processing flow:

- **Quality control**
- **Airborne and cosmic correction (IAEA, 2003)**
2013 survey data:
Used parameters: (determined by high altitude calibration flights near Langoya in July 2013)
Aircraft background counts:
K window 7
U window 0.9
Th window 0.9
Uup window 0
Total counts 36
Cosmic background counts (normalized to unit counts in the cosmic window):
K window 0.0617
U window 0.0454
Uup window 0.0423
Th window 0.0647
Total counts 1.0379

2014 survey data

Used parameters: (determined by high altitude calibration flights near Frosta in January 2014)

Aircraft background counts:

K window 5.3584
U window 1.427
Th window 0
Uup window 0.7051
Total counts 42

Cosmic background counts (normalized to unit counts in the cosmic window):

K window 0.057
U window 0.0467
Uup window 0.0448
Th window 0.0643
Total counts 1.0317

- **Radon correction using upward detector method (IAEA, 2003)**

Used parameters (determined from survey data over water and land):

a_u : 0.2316 b_u : 0.3197
 a_k : 0.8386 b_k : 0.8209
 a_T : 0.0585 b_T : 0.7983
 a_{TC} : 18.132 b_{TC} : 0
 a_1 : 0.060078 a_2 : 0.018348

- **Stripping correction (IAEA, 2003)**

2013 survey data

Used parameters (determined from measurements on calibrations pads at the NGU on May 6 2013):

a 0.049524
b -0.00169
g -0.00131
alpha 0.29698
beta 0.47138
gamma 0.82905

2014 survey data

Used parameters (determined from measurements on calibrations pads at the NGU on June 5 2014):

a 0.047186
b -0.00166
g -0.00145
alpha 0.305607
beta 0.484063
gamma 0.814612

- **Height correction to a height of 60 m**

2013 survey data

Used parameters (determined by high altitude calibration flights near near Frosta in January 2014):

Attenuation factors in 1/m:

K: -0.00888
U: -0.00653
Th: -0.00662
TC: -0.00773

2014 survey data

Used parameters (determined by high altitude calibration flights near near Frosta in January 2014):

Attenuation factors in 1/m:

K: -0.009523
U: -0.006687
Th: -0.007393
TC: -0.00773

Converting counts at 60 m heights to element concentration on the ground

Used parameters (determined from measurements on calibrations pads at the NGU on June 5 2014):

- **Sensitivity (elements concentrations per count):**

2013 survey data:

K: 0.007480 %/counts
U: 0.087599 ppm/counts
Th: 0.156147 ppm/counts

2014 survey data:

K: 0.007545 %/counts
U: 0.088909 ppm/counts
Th: 0.151433 ppm/counts

- **Microlevelling using Geosoft menu and smoothing by a convolution filtering**

Used parameters for microlevelling:

De-corrugation cutoff wavelength:	800 m
Cell size for gridding:	200 m
Naudy (1968) Filter length:	800 m

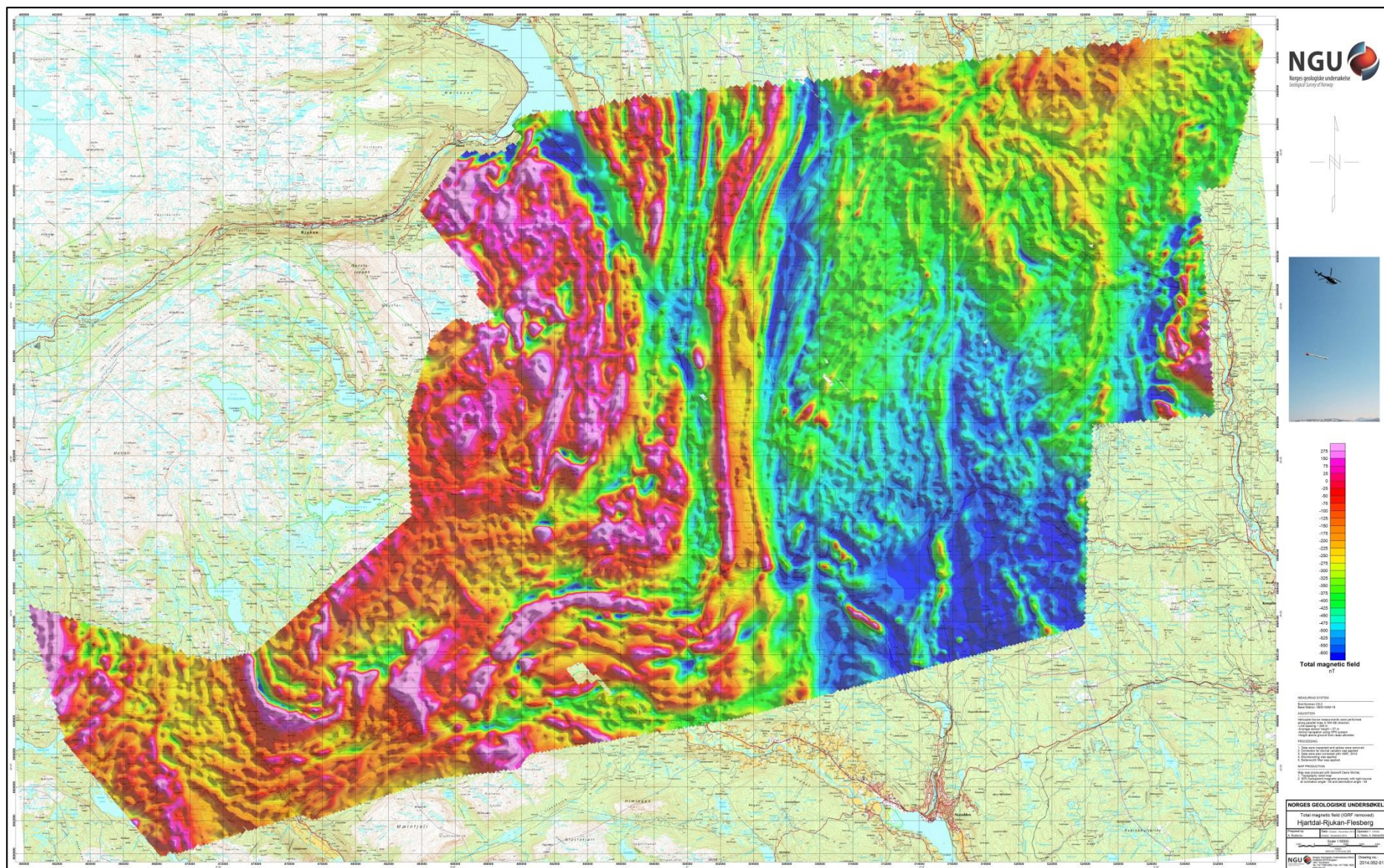


Figure 5: Total Magnetic Field

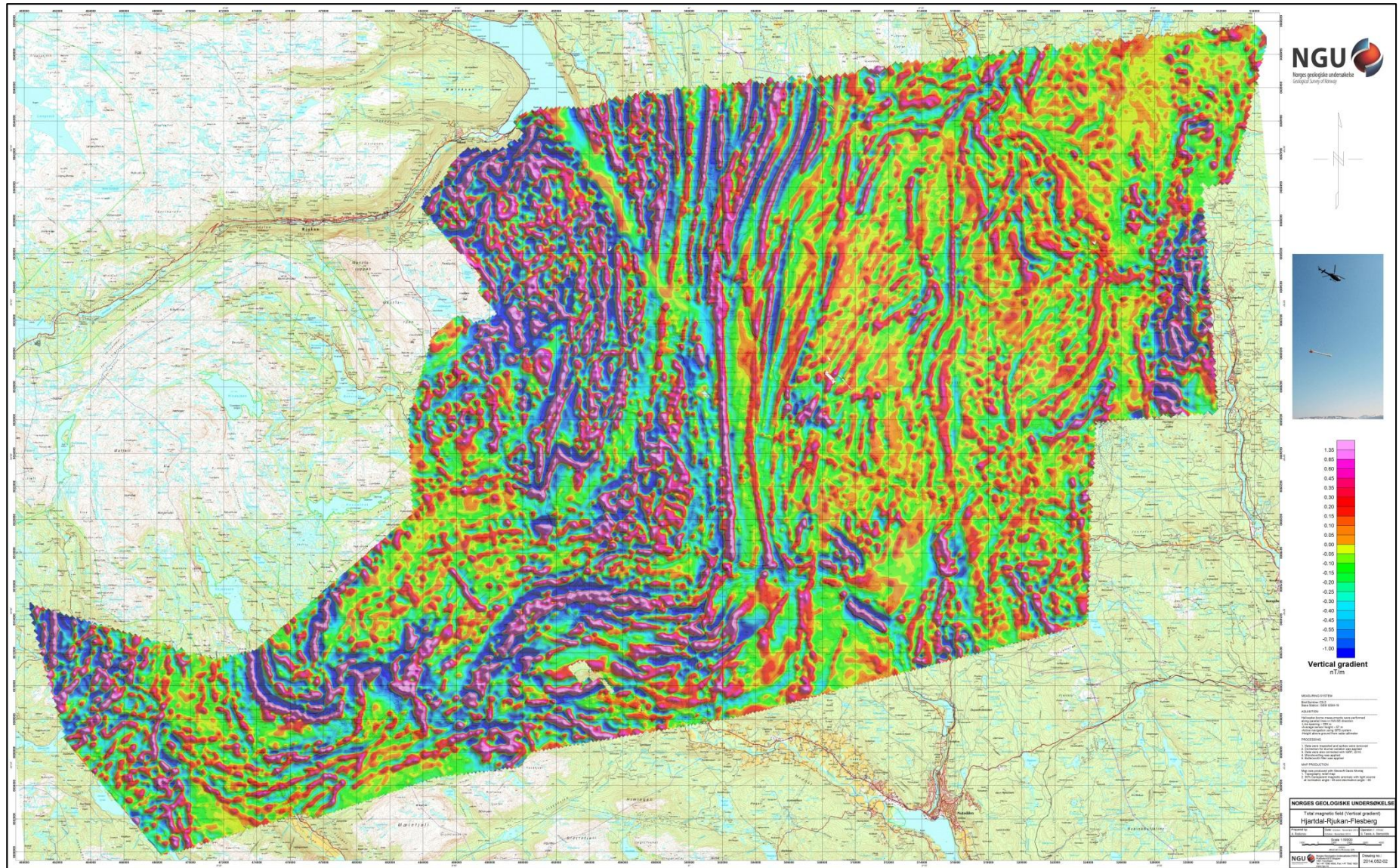


Figure 6: Magnetic Vertical Derivative

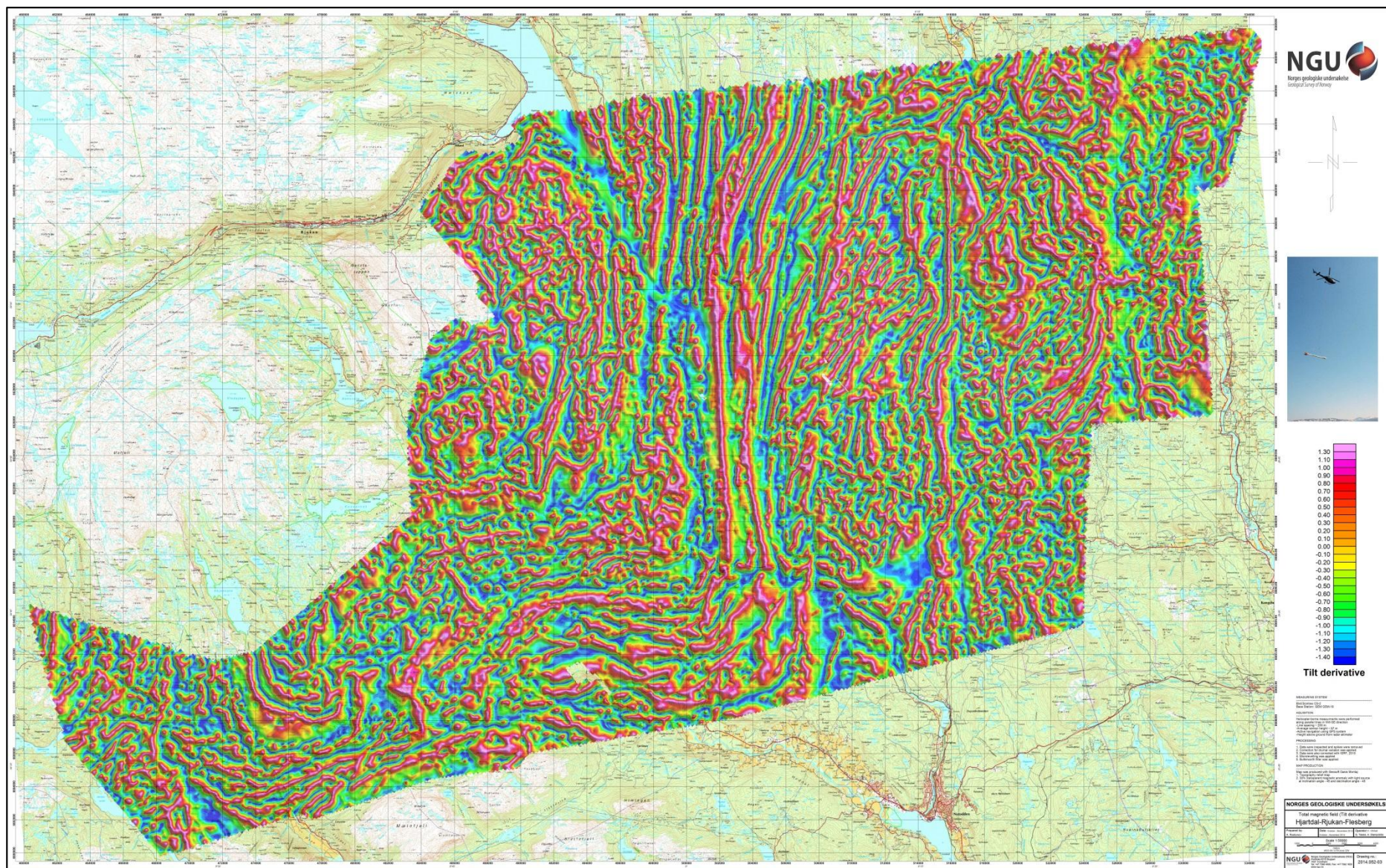


Figure 7: Magnetic Tilt Derivative

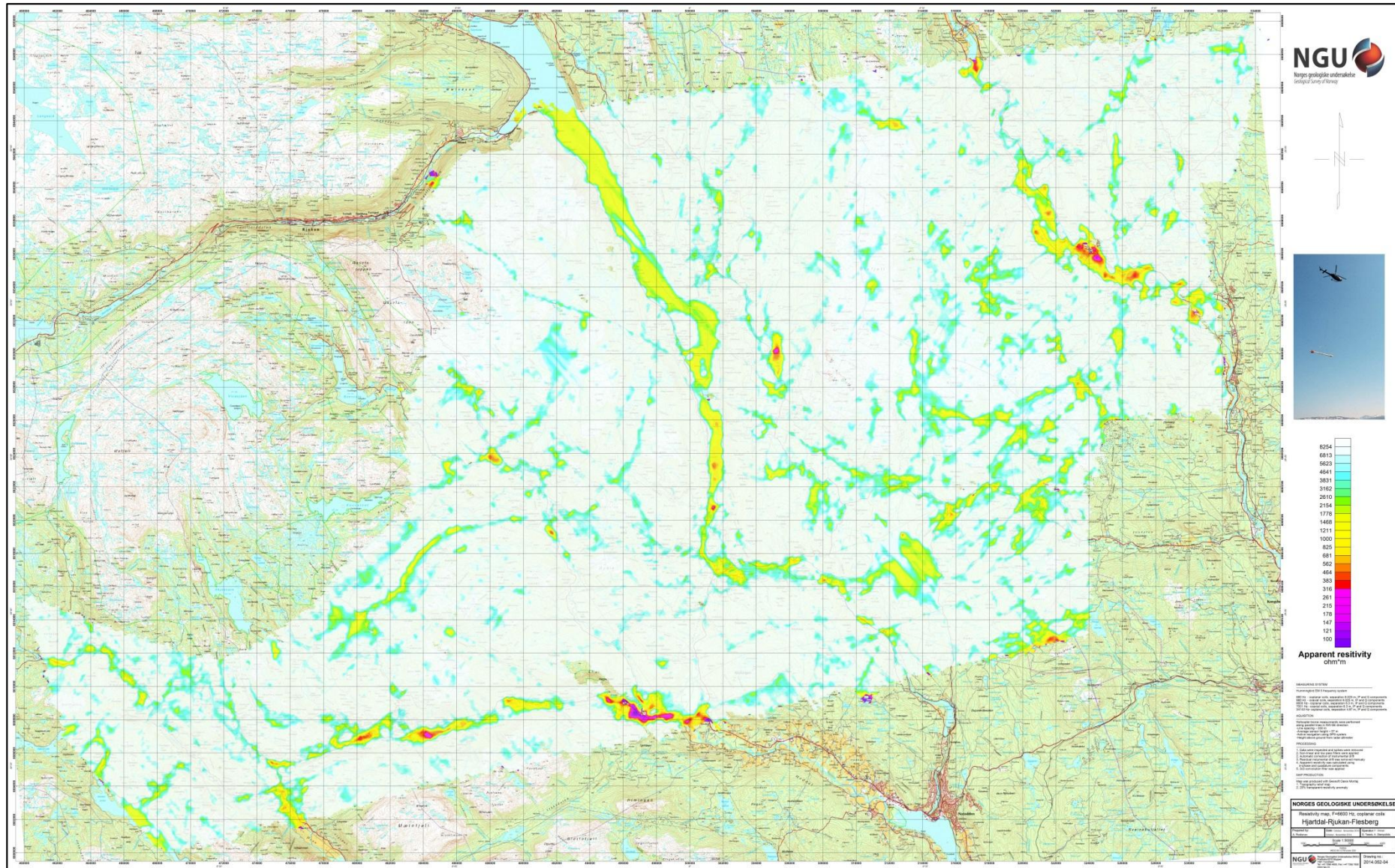


Figure 8: Apparent resistivity. Frequency 6600 Hz, Coplanar coils

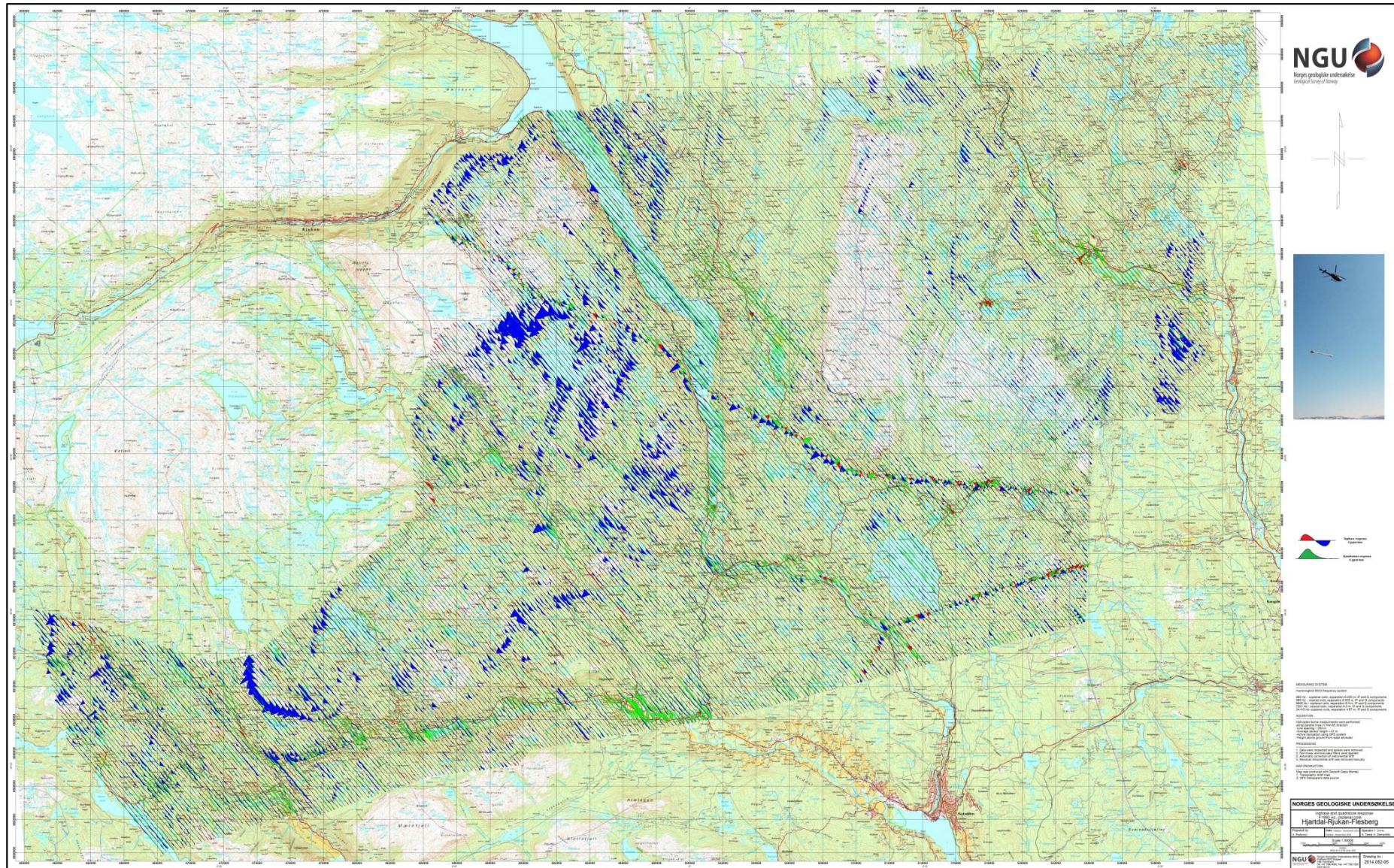


Figure 9: In-phase and quadrature response. Frequency 880 Hz, coplanar coils

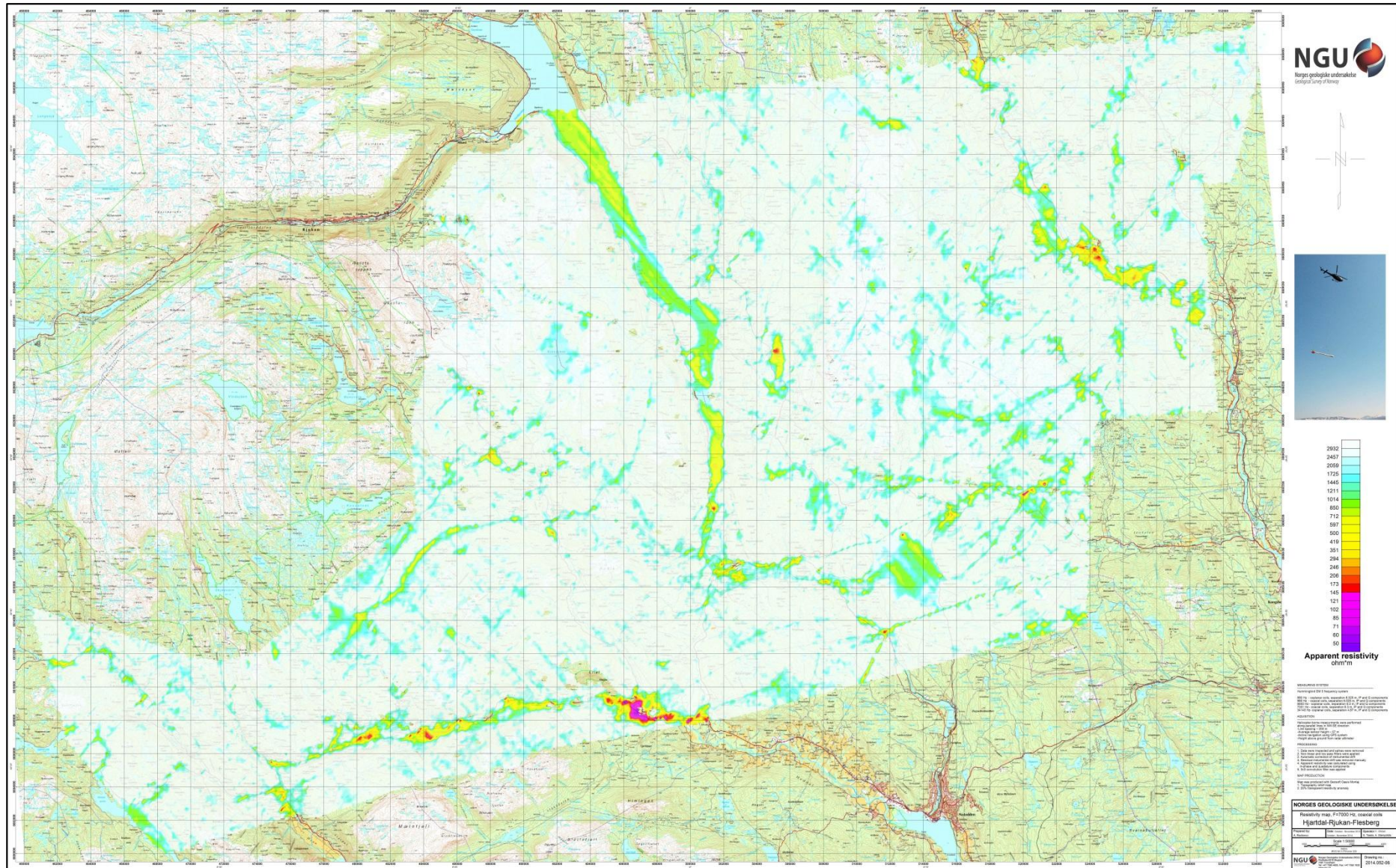


Figure 10: Apparent resistivity. Frequency 7000 Hz, Coaxial coils

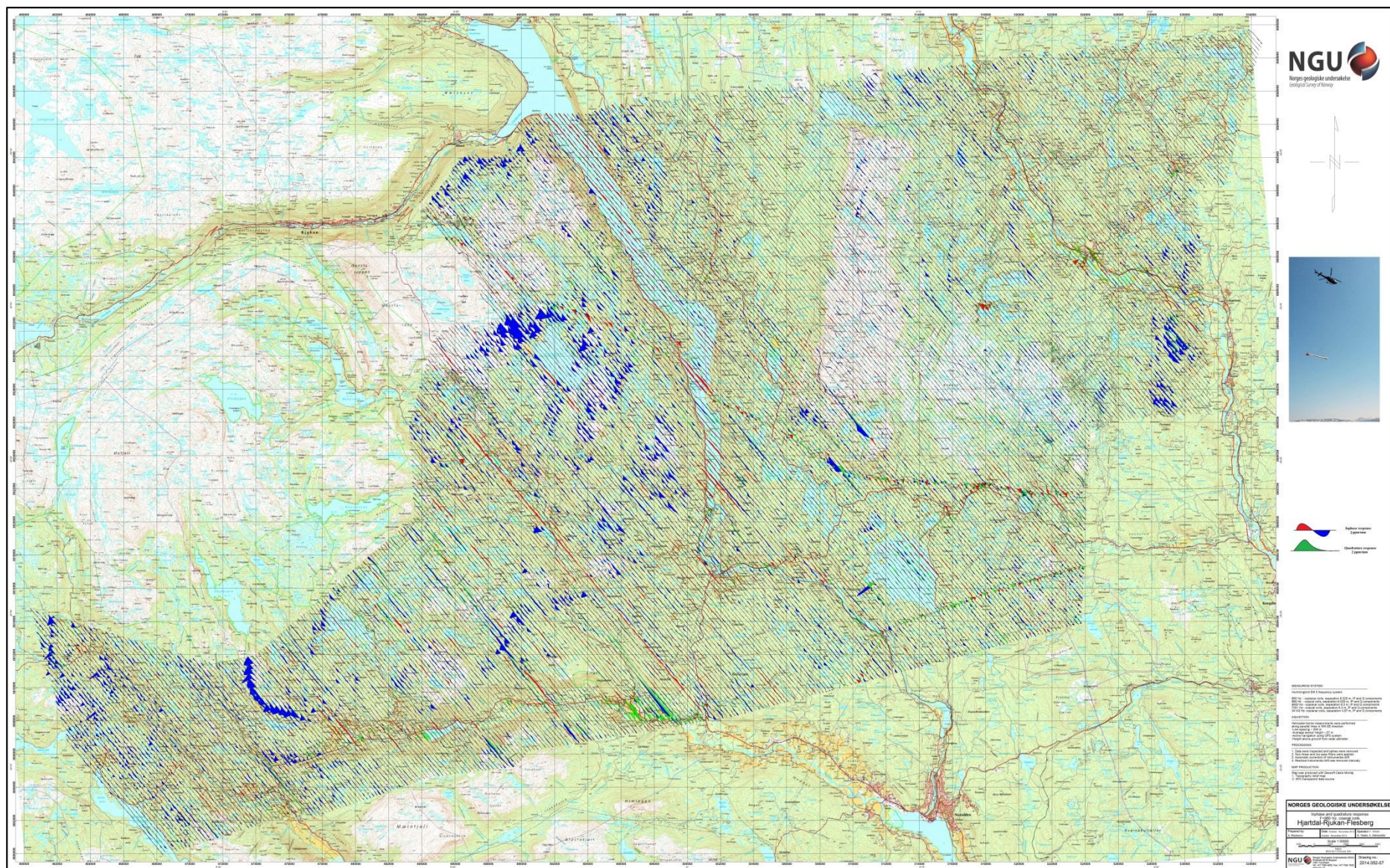


Figure 11: In-phase and quadrature response. Frequency 980 Hz, Coaxial coils

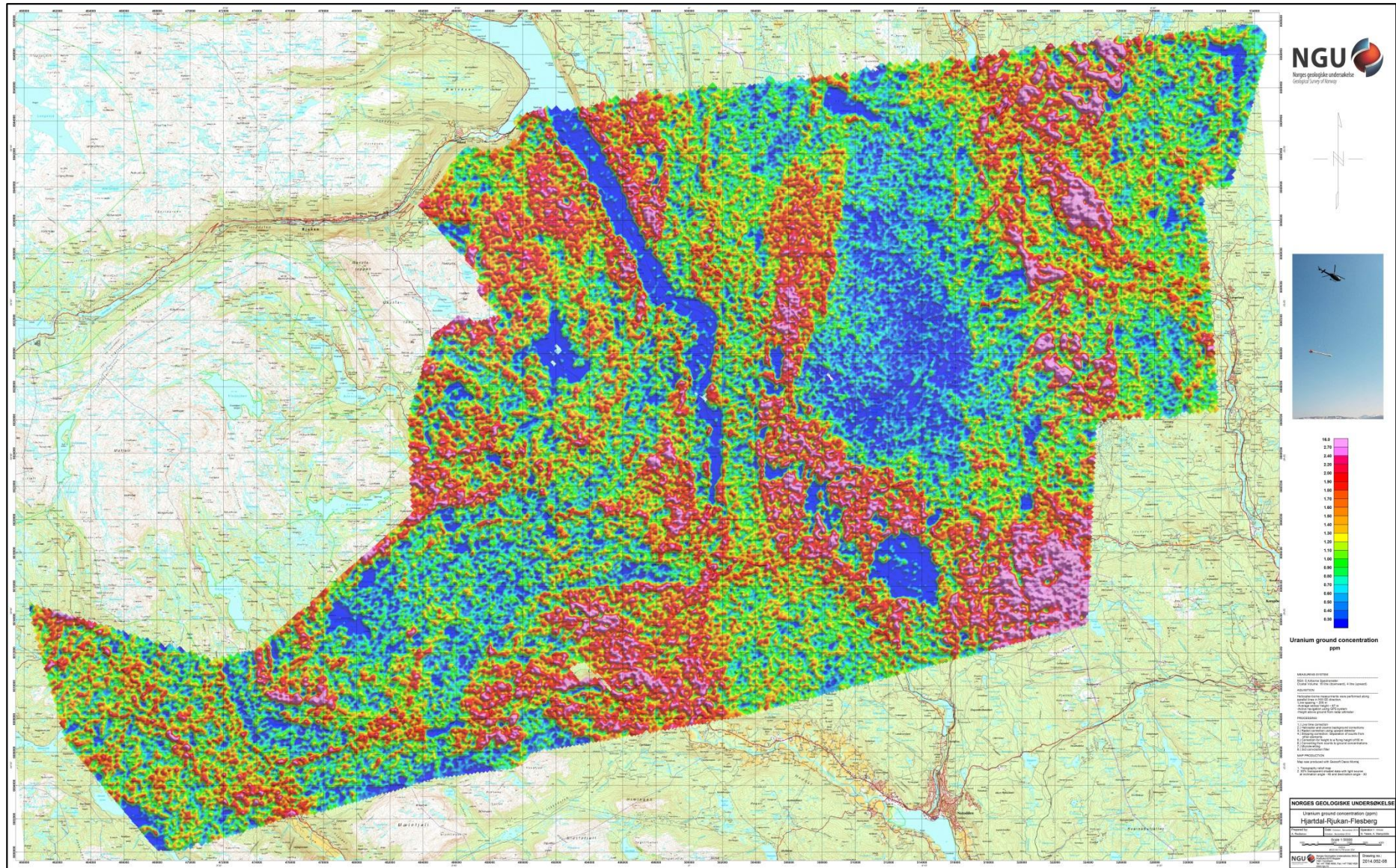


Figure 12: Uranium ground concentration

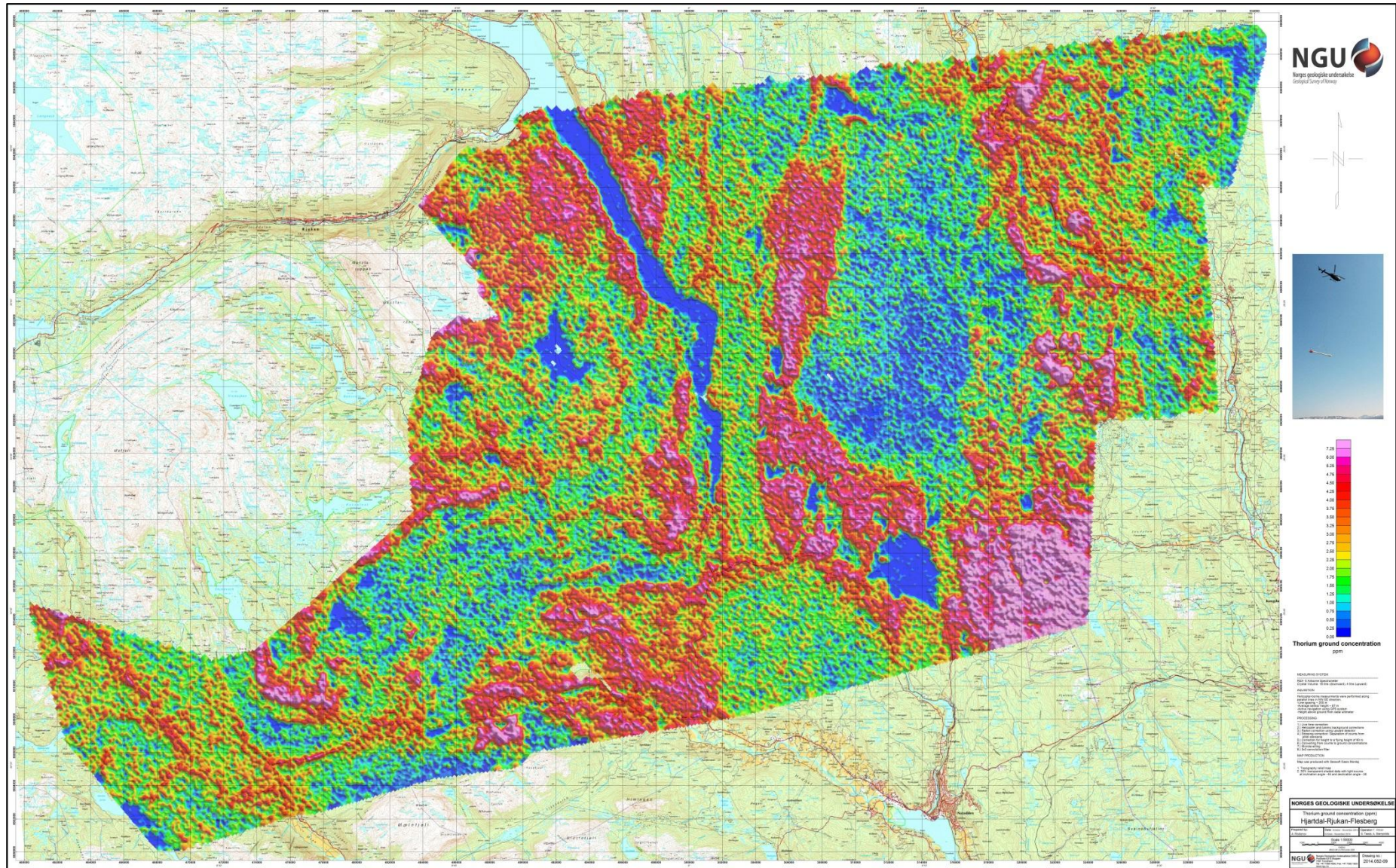


Figure 13: Thorium ground concentration

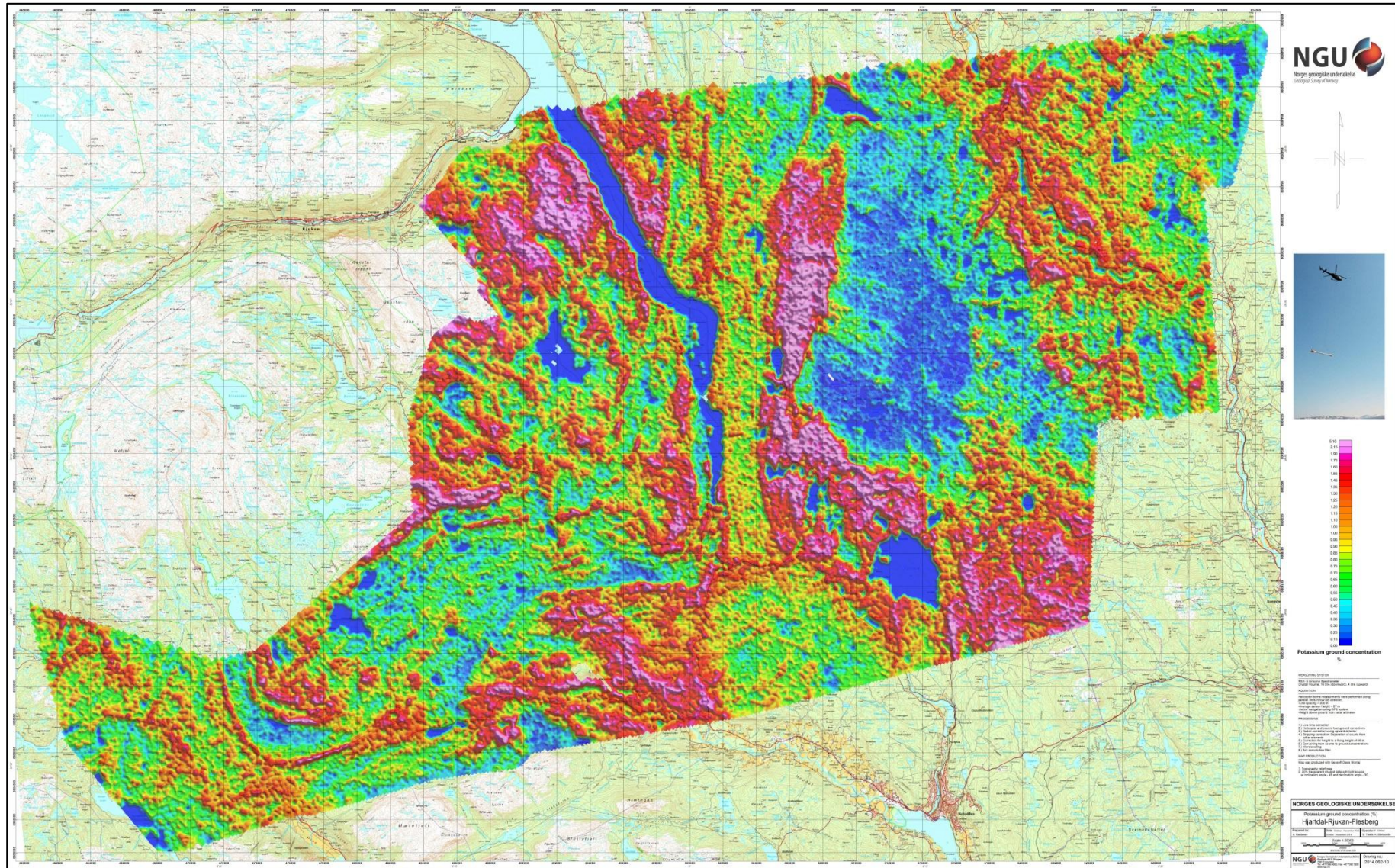


Figure 14: Potassium ground concentration

